tvst

Retina

Implications of Ocular Confounding Factors for Aqueous Humor Proteomic and Metabolomic Analyses in Retinal Diseases

Björn Titz[1,*], Juliane Siebourg-Polster[1,*], Francois Bartolo[1,2], Vincent Lavergne[1,3], Zhiwen Jiang[1], Javier Gayan[1], Lebriz Altay[4], Philip Enders[4], Christoph Schmelzeisen[5], Quynh-Trang Ippisch[5], Michael Janusz Koss[5], Siamak Ansari-Shahrezaei[6], Justus Gerhard Garweg[7,8], Sascha Fauser[1], and Andreas Dieckmann[1]

[1] Roche Pharmaceutical Research and Early Development, Roche Innovation Center Basel, F. Hoffmann-La Roche, Basel, Switzerland
[2] EFOR-CVO et Soladis, Champagne-au-Mont-d'Or, France
[3] EFOR-CVO et Soladis, Basel, Switzerland
[4] Department of Ophthalmology, Medical Faculty and University Hospital of Cologne, Cologne, Germany
[5] Eye Center Nymphenburger Höfe, Munich, Germany
[6] Karl Landsteiner Institute for Retinal Research and Imaging, Vienna, Austria
[7] Berner Augenklinik, Bern, Switzerland
[8] Department of Ophthalmology, Bern University Hospital, University of Bern, Bern, Switzerland

Correspondence: Andreas Dieckmann, Roche Pharmaceutical Research and Early Development, Roche Innovation Center Basel, F. Hoffmann-La Roche Ltd., Grenzacher Str. 124, Basel 4070, Switzerland. e-mail: andreas.dieckmann@roche.com

Received: February 27, 2024
Accepted: May 2, 2024
Published: June 24, 2024

Keywords: aqueous humor; biomarker; proteomics; metabolomics; confounders

Citation: Titz B, Siebourg-Polster J, Bartolo F, Lavergne V, Jiang Z, Gayan J, Altay L, Enders P, Schmelzeisen C, Ippisch QT, Koss MJ, Ansari-Shahrezaei S, Garweg JG, Fauser S, Dieckmann A. Implications of ocular confounding factors for aqueous humor proteomic and metabolomic analyses in retinal diseases. Transl Vis Sci Technol. 2024;13(6):17, https://doi.org/10.1167/tvst.13.6.17

Purpose: To assess the impact of ocular confounding factors on aqueous humor (AH) proteomic and metabolomic analyses for retinal disease characterization.

Methods: This study recruited 138 subjects (eyes): 102 with neovascular age-related macular degeneration (nAMD), 18 with diabetic macular edema (DME), and 18 with cataract (control group). AH samples underwent analysis using Olink Target 96 proteomics and Metabolon's metabolomics platform Data analysis included correlation, differential abundance, and gene-set analysis.

Results: In total, 756 proteins and 408 metabolites were quantified in AH. Total AH protein concentration was notably higher in nAMD (3.2-fold) and DME (4.1-fold) compared to controls. Pseudophakic eyes showed higher total AH protein concentrations than phakic eyes (e.g., 1.6-fold in nAMD) and a specific protein signature indicative of matrix remodeling. Unexpectedly, pupil-dilating drugs containing phenylephrine/tropicamide increased several AH proteins, notably interleukin-6 (5.4-fold in nAMD). Correcting for these factors revealed functionally relevant protein correlation clusters and disease-relevant, differentially abundant proteins across the groups. Metabolomics analysis, for which the relevance of confounder adjustment was less apparent, suggested insufficiently controlled diabetes and chronic hyperglycemia in the DME group.

Conclusions: AH protein concentration, pseudophakia, and pupil dilation with phenylephrine/tropicamide are important confounding factors for AH protein analyses. When these factors are considered, AH analyses can more clearly reveal disease-relevant factors.

Translational Relevance: Considering AH protein concentration, lens status, and phenylephrine/tropicamide administration as confounders is crucial for accurate interpretation of AH protein data

Introduction

The proximity of aqueous humor (AH) and vitreous humor (VH) to the retina makes them valuable matrices for unveiling disease mechanisms and identifying biomarkers and targets for retinal diseases. Although the collection of VH samples is typically restricted to vitreoretinal surgery due to the potential for severe vision-threatening complications,[1] sampling of AH via anterior chamber paracentesis is a well-established procedure with a low risk profile.[2,3] AH is separated from VH by the lens and other structures, but various studies have established associations between specific proteins found in AH and VH, suggesting that AH may reflect vitreous levels of these factors.[4–10] There are numerous examples where the detection of specific AH proteins has played a crucial role in enhancing our understanding of pharmacokinetics, pharmacodynamics, and pathophysiology of ocular diseases.[11–13] Expanding upon this, proteomic profiling employing liquid chromatography–mass spectrometry (LC/MS)-based technologies has enabled the detection of hundreds of proteins in AH samples.[14–21] Furthermore, the emergence of targeted, highly multiplex, and highly sensitive technologies, such as the Proximity Extension Assay (PEA) platform (Olink Proteomics AB, Uppsala, Sweden), allows the detection and relative quantification of low abundant proteins, including cytokines, chemokines, and growth factors.[22] Notably, the PEA technology can measure over 1000 proteins in a small sample volume of AH.[10] Several proteomic AH studies have already identified proteins that are associated with key biological processes.[14–19] Similarly, metabolomic analysis of AH has assessed conditions such as glaucoma, neovascular age-related macular degeneration (nAMD), and diabetic macular edema (DME) and has contributed to an increasing understanding of the pathogenesis of these diseases.[23–26]

However, confounding factors are relevant sources of bias and variability and are critical to consider to ensure correct data interpretation.[27,28] Previous research suggests that individuals with pseudophakic eyes have higher protein concentrations in the AH compared to those with phakic eyes.[29–32] Moreover, inflammatory processes in various diseases can lead to elevated AH protein levels which is often attributed to the breakdown of the blood–ocular barrier.[33–40]

Building on this work, the present study aimed to further assess the influence of total AH protein concentration and lens status, as ocular confounding factors, on the proteomic and metabolomic profiles of AH samples from patients with DME and nAMD. The goal was not only to use these insights to improve the accuracy of AH molecular signatures associated with the pathologies of nAMD and DME to enhance our understanding of the molecular changes associated with these diseases but also to potentially identify novel biomarkers for their diagnosis and candidate treatment targets.

Methods

Study and Patients

This work is part of a prospectively designed, cross-sectional study that was performed at four study sites: Department of Ophthalmology, University Hospital Cologne (Cologne, Germany), Berner Augenklinik (Bern, Switzerland), Karl Landsteiner Institute for Retinal Research and Imaging (Vienna, Austria), and Eye Center Nymphenburger Höfe (Munich, Germany). The study protocol was conducted in accordance with the tenets of the Declaration of Helsinki and was approved by the ethics committees of the respective sites. Signed informed consent was obtained from each patient prior to participation.

To be eligible, patients had to have active nAMD or DME in the study eye undergoing anti-vascular endothelial growth factor (anti-VEGF) intravitreal treatment (IVT), as well as otherwise healthy controls (without any systemic or local medication) undergoing surgery for senile cataract. Exclusion criteria included any previous ophthalmic surgery except for previous cataract removal in the nAMD/DME group, any ocular retinal laser treatment within the previous 3 months, laser iridotomy or yttrium aluminum garnet (YAG) laser capsulotomy within the previous month, uncontrolled glaucoma, intraocular inflammation, or chronic systemic inflammatory diseases such as diabetes mellitus (except in the DME group), autoimmune disease, or cancer and corresponding therapies as determined by the medical history. Patients treated for dry eye disease in the month prior to AH sampling (except for lubricants), with intra-/periocular steroids in the previous 6 months, or with systemic corticosteroids in the previous week were also excluded. In the control (i.e., cataract) group, the exclusion criteria also included any history of retinal disease. Clinical data were extracted from electronic patient records.

Sample Collection

AH was collected via anterior chamber paracentesis for all patients. Paracentesis was performed using a sterile 30-gauge needle on a 1-mL syringe, and approximately 100 µL of AH was collected. Paracentesis was performed at the time of cataract surgery for the

control group and immediately before anti-VEGF IVT in the nAMD and DME groups. Following collection, aqueous samples were stored within 15 minutes at −80°C until sample shipment to the analytical labs.

Proteomic Measurement

AH samples (25 µL each) were shipped on dry ice to Olink Proteomics AB (Uppsala, Sweden) and analyzed using the Olink Target 96 platform. A single measurement was performed for each sample. The following 13 panels were assessed by Olink: cardiometabolic panel, cell regulation panel, cardiovascular II panel, cardiovascular III panel, development panel, immune response panel, inflammation panel, metabolism panel, neurology panel, neuro-exploratory panel, oncology II panel, oncology III panel, and organ damage panel. A full list of the proteins in the selected panels is available in Supplementary Table S1. Protein levels were measured on a relative scale and presented as the normalized protein expression (NPX), which is an arbitrary unit on a $\log_2$ scale.

Total AH protein concentrations were determined using the NanoOrange Protein Quantitation Kit (#N-6666; Thermo Fisher Scientific, Waltham, MA) according to the manufacturer's instructions. Quality checks for the Olink proteomics data included detectability, plate effects, and outlier identification. Olink establishes a detection threshold for each protein (limit of detection [LOD]), informed by the background signal in negative controls. Despite this, the Olink dataset reports NPX values for readings that fall below the LOD. Other random missing values, which were sparse and resulted from technical issues, were deemed negligible and did not influence the statistical evaluation. Proteins with sparse detectability, defined as those detected in less than 30% of samples with NPX values above the LOD, were omitted from the statistical analysis through a data curation step. Nonetheless, analytes with significant differential detectability in any of the disease groups were kept, even if detected in less than 30% of samples (Fisher's exact test, false discovery rate [FDR] < 0.01). For the remainder of the proteins, NPX values below the LOD were kept as the best available estimates for their protein abundances.

Metabolomic Measurement

AH samples (25 µL each) were shipped on dry ice to Metabolon. (Morrisville, NC) and analyzed using Metabolon's HD4 Global Metabolomics platform. Peak area values obtained from Metabolon were $\log_2$ transformed. Quality checks for the Metabolon metabolomics data included detectability and outlier identification. Metabolites detected in less than 30% of samples were omitted from the statistical analysis. Nonetheless, analytes with significant differential detectability in any of the disease groups were kept, even if detected in less than 30% of samples (Fisher's exact test, FDR < 0.01). For the remainder, a bimodal imputation strategy was used: Metabolites with missing values in ≤2% of the samples were treated as missing at random and the median of the metabolite was used; otherwise, the missing values were treated as left censored (<LOD) and imputed as the minimum value divided by two.[41] Finally, the quantification values were scaled for the input sample volume.

Statistical Analysis

Differential abundance between conditions was assessed using contrasts in the context of linear models using the limma package in R (R Foundation for Statistical Computing, Vienna, Austria).[42] Covariates were included for the specific comparisons as described in the text. Moderated *t*-tests were then performed using the empirical Bayes method. The resulting *P* values were adjusted for multiple testing using the Benjamini–Hochberg method to control the false discovery rate (FDR). Analytes with an adjusted *P* value below a specified threshold (set at 0.05) were considered differentially expressed.

The relationship between AH protein concentration and the study group and lens status was assessed using a linear modeling approach. To satisfy the assumption of normality, protein concentration data were $\log_2$ transformed. The linear model included study group and lens status and their interaction as predictor variables, with the transformed protein concentration as the response variable. Differences were examined using the estimated marginal means method,[43] which facilitated the statistical analysis of specific contrasts, including the overall effect of the study group, study group by lens status effect, and lens status by study group effect. The model accounted for the varying cell frequencies by applying weights to the data. Significance levels for the resulting *P* values were controlled using Tukey's method for multiple comparisons and further cross-adjusted with the Bonferroni correction.

Pairwise correlation matrices were calculated using the Spearman method. Matrices were calculated for all samples and for each study group (i.e., controls, nAMD, and DME). Non-adjusted and data fully adjusted for the lens status, 3-hydroxymandelate exposure, protein concentration, and study group were considered. Data matrix adjustment was performed by fitting a linear model of the considered covariates and subtracting these model estimates (without intercept) from the original data matrices, following the

approach taken by the removeBatchEffect function of the limma package in R.[42] Consensus clusters were identified with the ConsensusClusterPlus package in R[44] using *k*-means clustering on Euclidean distance with 20 subsamples. The number of considered cluster *k* was chosen based on the "delta area plot" method, in which a *k* was chosen at which no appreciable further increase in the area under the cumulative distribution function curve was observed.[45]

For gene-set enrichment analysis (GSEA) and overrepresentation analysis (ORA), two sources of gene-set collections were considered. Using the msigdbr package in R, C2CP gene sets from the MSigDB database were obtained (Reactome, Kyoto Encyclopedia of Genes and Genomes [KEGG], and general subsets).[46,47] From the StringDB, we considered the WikiPathway, Reactome Pathway, local network cluster (STRING), and biological process (Gene Ontology [GO]) gene-set collections.[48] Fast GSEA was performed using the piano package in R with the $\log_2$ fold change from baseline as protein-level statistics.[49] ORA was performed with a one-tailed Fisher's exact test using the piano package in R. FDR-adjusted $P < 0.05$ was considered significant. In addition, genes associated with diabetic retinopathy (DR) or AMD were obtained from the Open Targets database.[50]

Results

Study Population and Sample Analyses

The study included a total of 138 patients: 102 with nAMD, 18 with DME, and 18 with cataract (i.e., controls). Patients undergoing IVT received aflibercept (62% of nAMD and 56% of DME) or bevacizumab (31% of nAMD and 28% of DME), with the remainder treated with ranibizumab or multiple IVT drugs. Further patient characteristics can be found in the Table.

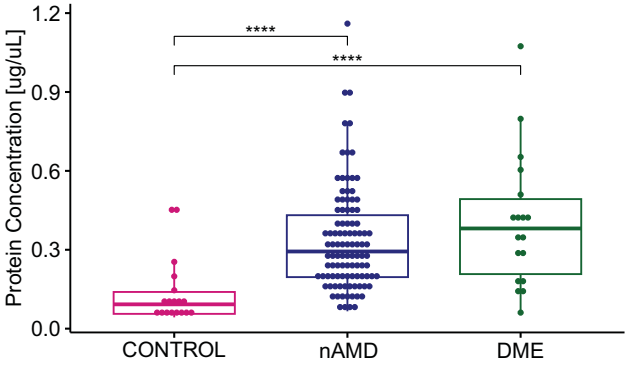

Figure 1. Protein concentrations in AH samples from the nAMD, DME, and control groups. Box plots represent the protein concentrations in the AH samples across the three groups. Individual patient data points are shown. Statistically significant differences between groups are denoted by asterisks, as determined by a linear model and estimated marginal means contrasts (*$P < 0.05$, **$P < 0.01$, ***$P < 0.001$, ****$P < 0.0001$, Tukey adjusted and Bonferroni cross-adjusted).

For protein measurements, we employed the Olink Target 96 platform. Of 1161 unique proteins across 13 distinct panels in the Olink Target 96 platform, 756 were detected in more than 30% of the samples after stringent quality-control measures. For the metabolite profiling, we utilized Metabolon's liquid chromatography–tandem mass spectrometry (LC-MS/MS) platform. Of >1000 small-molecule metabolites, 408 were reliably quantified using a detection threshold of 30%.

Elevated Aqueous Humor Protein Concentration in Disease

AH samples from patients with nAMD and patients with DME demonstrated significantly elevated total protein concentrations (Fig. 1): 0.092 ± 0.057 µg/µL (median ± mean absolute deviation) for controls, 0.294 ± 0.152 µg/µL for nAMD ($P < 0.0001$ vs. controls), and 0.381 ± 0.243 µg/µL for DME ($P < 0.0001$ vs. controls).

Table. Patient Characteristics

Characteristic	Controls ($n = 18$)	nAMD ($n = 102$)	DME ($n = 18$)
Sex, *n* (%)			
Female	11 (61)	54 (53)	8 (44)
Male	7 (39)	48 (47)	10 (56)
Age (y), median (IQR)	73 (70–80)	79 (74–83)	69 (62–71)
Lens status, *n* (%)			
Phakic	18 (100)	24 (24%	8 (44)
Pseudophakic	0 (0)	78 (76)	10 (56)

IQR, interquartile range.

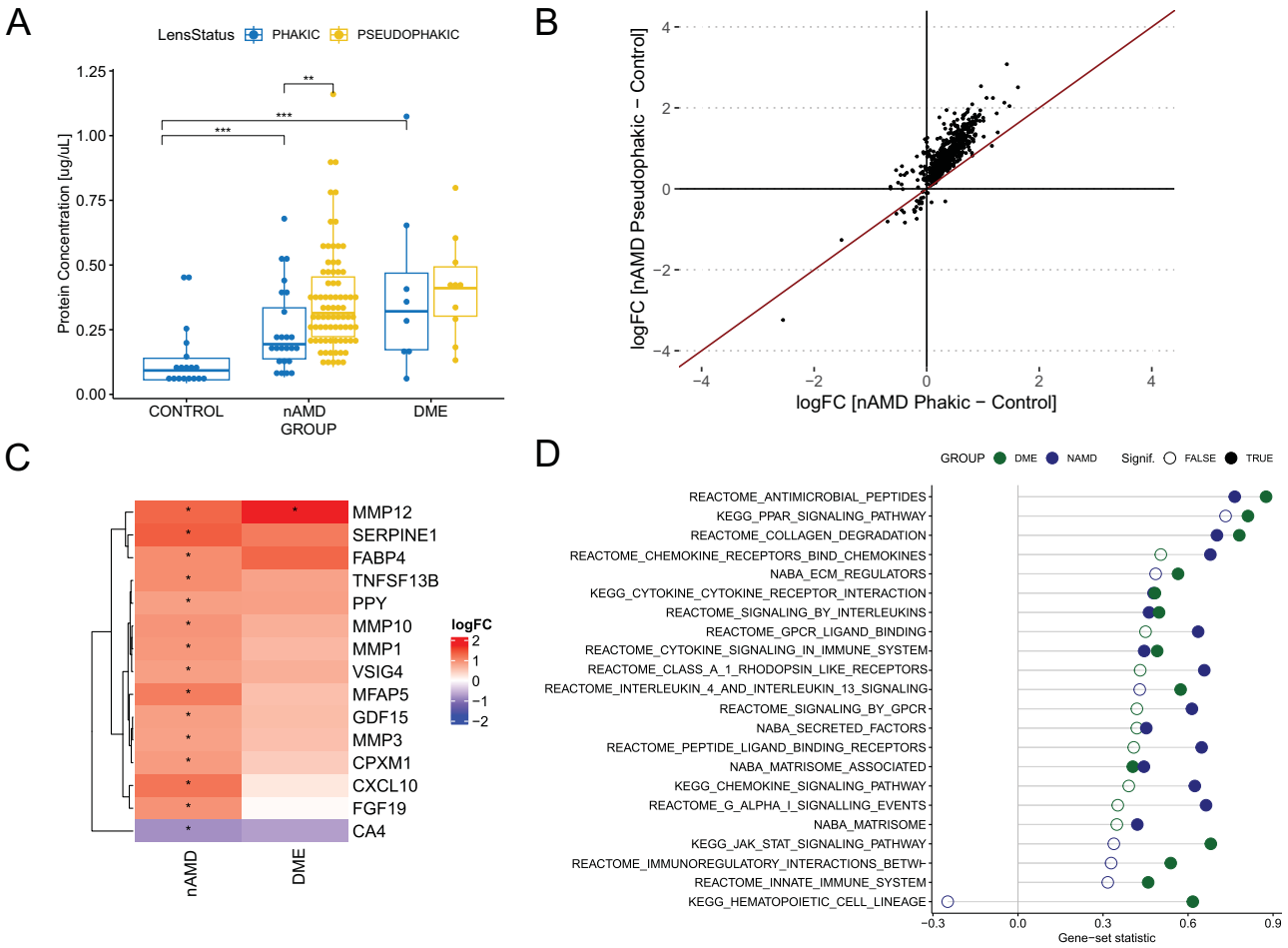

Figure 2. Influence of lens status on aqueous humor protein profiles. (**A**) Box plots illustrate the distribution of protein concentrations in AH samples across the three groups categorized by lens status. Individual patient data points are shown. Statistically significant differences are highlighted with asterisks, as determined by a linear model and estimated marginal means contrasts (*$P < 0.05$, **$P < 0.01$, ***$P < 0.001$, Tukey adjusted and Bonferroni cross-adjusted). (**B**) A scatterplot shows the $\log_2$ fold changes (logFC) for AH proteins between phakic nAMD and controls (*x*-axis) and pseudophakic nAMD and controls (*y*-axis). Each point represents an individual AH protein, with the *red line* indicating equivalence in $\log_2$ fold change between phakic and pseudophakic conditions. (**C**) A heatmap displays the differential abundance of proteins, adjusted for protein concentration, between pseudophakic and phakic eyes within the nAMD and DME patient groups. The $\log_2$ fold changes are visualized with a *color gradient*, and proteins with statistically significant differences are marked (*$P < 0.05$, FDR-adjusted). The heatmap is confined to the top 15 proteins ranked by the absolute value of logFC. (**D**) Results from GSEA for lens status (pseudophakic vs. phakic) are presented. Significantly enriched gene sets from the mSigDB C2CP collection are indicated (*$P < 0.05$, FDR-adjusted). The *dots* show the gene-set statistics, color-coded by patient group (DME in *green* and nAMD in *blue*), and *filled dots* represent statistically significant enrichments.

Lens Status Impact on Aqueous Humor Protein Concentration and Composition in Retinal Disease

Our analysis of AH samples from the nAMD cohort revealed a significant elevation (+62%) in protein concentrations in pseudophakic eyes compared to phakic eyes ($P < 0.01$) (Fig. 2A): 0.314 ± 0.148 µg/µL for pseudophakic and 0.194 ± 0.100 µg/µL for phakic eyes of patients with nAMD. Although a similar trend was observed in the DME group, with pseudophakic eyes exhibiting a higher median protein concentration than phakic eyes, the differences did not reach statistical significance, possibly due to the smaller sample size in this subgroup (Supplementary Fig. S1). Of note, compared with phakic eyes of the control group (0.092 ± 0.057 µg/µL), phakic eyes of patients with nAMD (0.194 ± 0.100 g/µL) and DME (0.321 ± 0.230 µg/µL) showed two- and threefold (for nAMD and DME, respectively) higher protein concentrations ($P < 0.001$). Note that the AH protein concentration in nAMD did not substantially change with time since diagnosis (Supplementary Fig. S2).

To further dissect the impact of lens status on individual AH proteins, we compared the levels of these proteins in patients with nAMD with pseudophakic and phakic eyes to those in controls, who were all phakic at the time of sample collection (Fig. 2B). The analysis revealed a general upward shift in the $\log_2$ fold changes for the pseudophakic nAMD versus control group comparison, suggesting that the presence of a pseudophakia may literally "amplify" the differences in protein concentrations associated with nAMD when compared to controls.

We also investigated whether specific functional protein categories were associated with lens status. A differential abundance analysis within the nAMD group, controlling for protein concentration as a covariate, revealed a positive association between pseudophakia and several proteins involved in the extracellular matrix remodeling, such as matrix metalloproteinase 1 (MMP1), MMP3, MMP10, MMP12, serpin family E member 1 (SERPINE1), and microfibril associated protein 5 (MFAP5), and signaling mediators, including growth differentiation factor 15 (GDF15), C-X-C motif chemokine ligand 10 (CXCL10), and fibroblast growth factor 19 (FGF19), as shown in Figure 2C (Supplementary Table S2). Conversely, carbonic anhydrase 4 (CA4) was negatively associated with pseudophakia.

GSEA corroborated these findings, indicating that gene sets related to the extracellular matrix (e.g., Reactome collagen degradation, Naba matrisome associated) and intercellular signaling (e.g., KEGG cytokine–cytokine receptor interaction, Reactome signaling by interleukins) were upregulated in both nAMD and DME groups in relation to lens status (Fig. 2D, Supplementary Table S3).

Influence of Pupil-Dilating Drugs on Aqueous Humor Protein Profiles

In an initial differential abundance analysis, interleukin-6 (IL-6) levels were unexpectedly higher in the control group than in the nAMD and DME groups (Fig. 3A). To explore this further, we stratified the control group into high and low IL-6 level groups using the median IL-6 level of the nAMD group as a cutoff (Fig. 3A). Metabolite differential abundance analysis between these two groups identified three metabolites—3-hydroxymandelate, *N*-lactoyl isoleucine, and *N*-lactoyl leucine—with significantly higher levels in the high IL-6 control group (Fig. 3B). Although we could not directly explain the latter two metabolites, we noticed that 3-hydroxymandelate represents the major metabolite of phenylephrine,[51] which is used primarily for its mydriatic (i.e., pupil-dilating) effect. Supporting this association between phenylephrine and 3-hydroxymandelate, these two analytes showed a strong correlation in AH (R^2 = 0.76, Spearman correlation) (Fig. 3C). However, phenylephrine was quantified below the quantification threshold in more samples than 3-hydroxymandelate, which likely resulted in a weaker association between IL-6 and phenylephrine than between IL-6 and 3-hydroxymandelate.

In addition, 34% of the patients with nAMD also exhibited elevated 3-hydroxymandelate levels above the quantification threshold, possibly depending on the dose and timing of dilating eye drops relative to the time of AH sampling (Fig. 3D). To investigate whether this observed exposure was associated with a similar effect on AH biomarkers in the nAMD as in the control group, we conducted a differential expression analysis, dividing the nAMD group based on low or high 3-hydroxymandelate levels, with the cutoff set based on the quantification threshold (Fig. 3E, Supplementary Table S4). Consistent with the control group findings, IL-6 was significantly upregulated in patients with nAMD with high 3-hydroxymandelate levels. In addition to IL-6, ezrin, granulocyte colony-stimulating factor (G-CSF/CSF3), the IL-6 family cytokine oncostatin M (OSM), and the tissue repair factor amphiregulin were significantly elevated in the high 3-hydroxymandelate group (Fig. 3F).

GSEA confirmed the biological impact of phenylephrine/3-hydroxymandelate exposure, with notable enrichment in the Reactome interleukin-6 family signaling gene set, among others related to cytokine signaling (Fig. 3G, Supplementary Table S5). Although the DME group included only two cases with elevated 3-hydroxymandelate levels, the gene-set responses, including those for IL-6 signaling, paralleled those observed in the control and nAMD groups.

In summary, our data show that phenylephrine/3-hydroxymandelate exposure is associated with increased IL-6 levels in AH.

Effect of Covariate Adjustment on Aqueous Humor Protein Correlations

We next assessed the impact of the identified ocular confounders on the correlation of AH proteins. Figure 4A displays the correlation heatmaps for AH proteins across study groups, where a generally strong positive correlation is indicated by the prevalent red hue, likely due to the association with total protein concentration and other confounders.

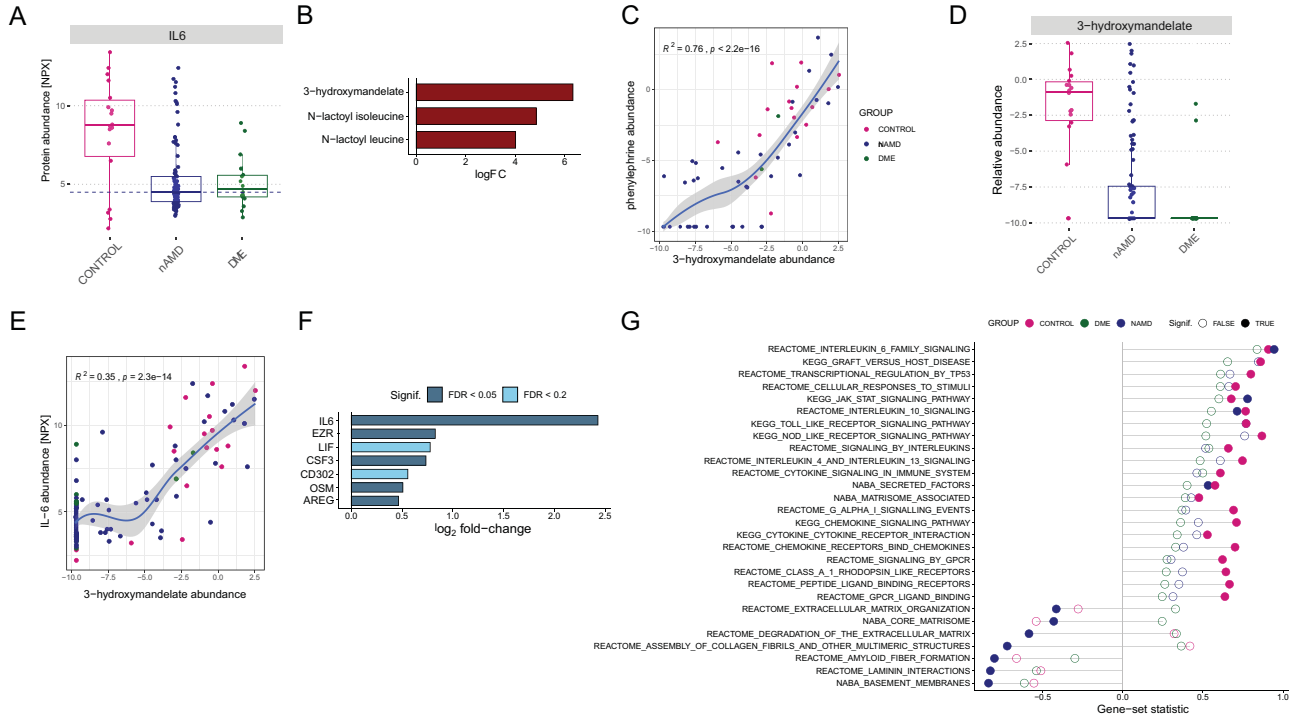

Figure 3. Association of phenylephrine/3-hydroxymandelate exposure with AH protein profiles. (**A**) Box plots display the relative protein abundance values (NPX) for IL-6 across the three patient groups, with individual data points superimposed for detailed visualization. The *dotted line* represents the threshold used to split the control group for subsequent differential abundance analysis. (**B**) Bar plot of the metabolites significantly associated with high versus low IL-6 levels within the control group (FDR $<$ 0.05). (**C**) Correlation between 3-hydroxymandelate and phenylephrine levels. Groups are *color coded*. A local polynomial regression curve (*blue*) with 95% confidence intervals (*gray areas*) is included. The Spearman coefficient of determination (R^2) and *P* are shown. (**D**) Box plots display the relative metabolite abundance values for 3-hydroxymandelate across the three patient groups, with individual data points superimposed for detailed visualization. For subsequent differential abundance analysis, the nAMD group was split at a relative quantity slightly above LOD (–9.5). (**E**) As in (**C**) but for the correlation between 3-hydroxymandelate and IL-6 levels. (**F**) Bar plot of the proteins associated with high versus low 3-hydroxymandelate levels in the nAMD group, with $\log_2$ fold changes indicated and significance levels represented by the *color scale*. (**G**) GSEA results for high versus low 3-hydroxymandelate levels in the nAMD group are shown. Significantly enriched gene sets from the mSigDB C2CP collection are marked (FDR $<$ 0.05). *Dots* correspond to gene-set statistics, with patient groups denoted by color (DME in *green*, nAMD in *blue*, and controls in *pink*), and *filled dots* indicate statistically significant gene sets.

Adjusting for protein concentration, lens status, and phenylephrine exposure revealed more distinct protein clusters (Fig. 4B). Consensus clustering, a resampling-based method, was utilized to assign proteins to clusters and assess cluster stability (Supplementary Fig. S3, Supplementary Table S6). This identified seven clusters in the control group and 10 in the nAMD and DME groups. Notably, shared clusters between nAMD and DME groups were found, with gene-set analysis indicating biological categories related to these clusters (Figs. 4C, 4D; Supplementary Tables S7A, S7B, S7C). For example, neuronal proteins were enriched in one cluster pair (nAMD cluster 1 and DME cluster 3) and metabolic enzymes in another (nAMD and DME cluster 8).

In conclusion, the identified confounding factors are important to consider when analyzing protein correlations in AH.

Impact of Covariate Adjustment on Differential Protein Abundance Analysis

Finally, we investigated how ocular confounders influence differential protein abundance analyses. Unadjusted comparisons between nAMD and DME groups versus the control group showed a majority of proteins were significantly upregulated (FDR $<$ 0.05) (Fig. 5A, Supplementary Table S8). Adjusting for lens status, protein concentration, and 3-hydroxymandelate exposure strongly reduced the number of differentially abundant proteins in nAMD versus controls (from 610 to 47) and DME versus controls (from 639 to 146) (Fig. 5B). Conversely, the DME versus nAMD comparison showed an increase in differentially abundant proteins from 35 to 72 upon adjustment. This is likely due to the smaller differences in confounders between the two retinal disease groups compared to the control

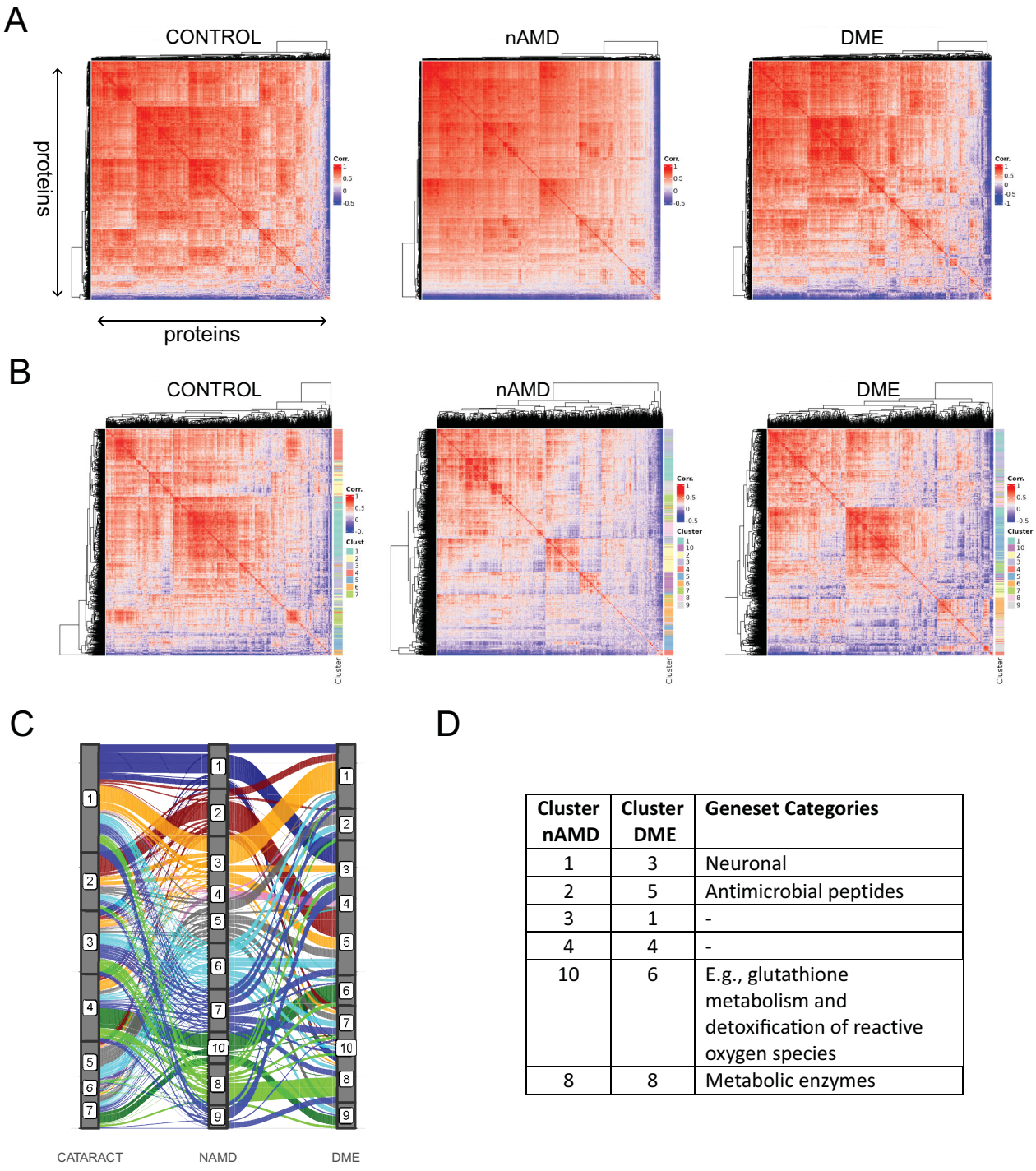

D

Cluster nAMD	Cluster DME	Geneset Categories
1	3	Neuronal
2	5	Antimicrobial peptides
3	1	-
4	4	-
10	6	E.g., glutathione metabolism and detoxification of reactive oxygen species
8	8	Metabolic enzymes

Figure 4. Impact of confounder adjustment on AH protein correlation patterns. (**A**) Heatmap showing Spearman correlation coefficients between protein pairs for each study group, with color intensity reflecting correlation strength. Proteins are hierarchically clustered on both axes. (**B**) Similar heatmap post-adjustment for protein concentration, lens status, and phenylephrine exposure, with cluster assignments denoted by the *color scale* on the right. (**C**) Alluvial plot depicting cluster assignment correspondence among groups, with cluster numbers labeled. Lines represent proteins and their respective clusters, with color reflecting nAMD group cluster assignments. (**D**) Table highlighting shared clusters between nAMD and DME groups, including a summary of gene-set analysis results. Detailed information is available in Supplementary Table S7.

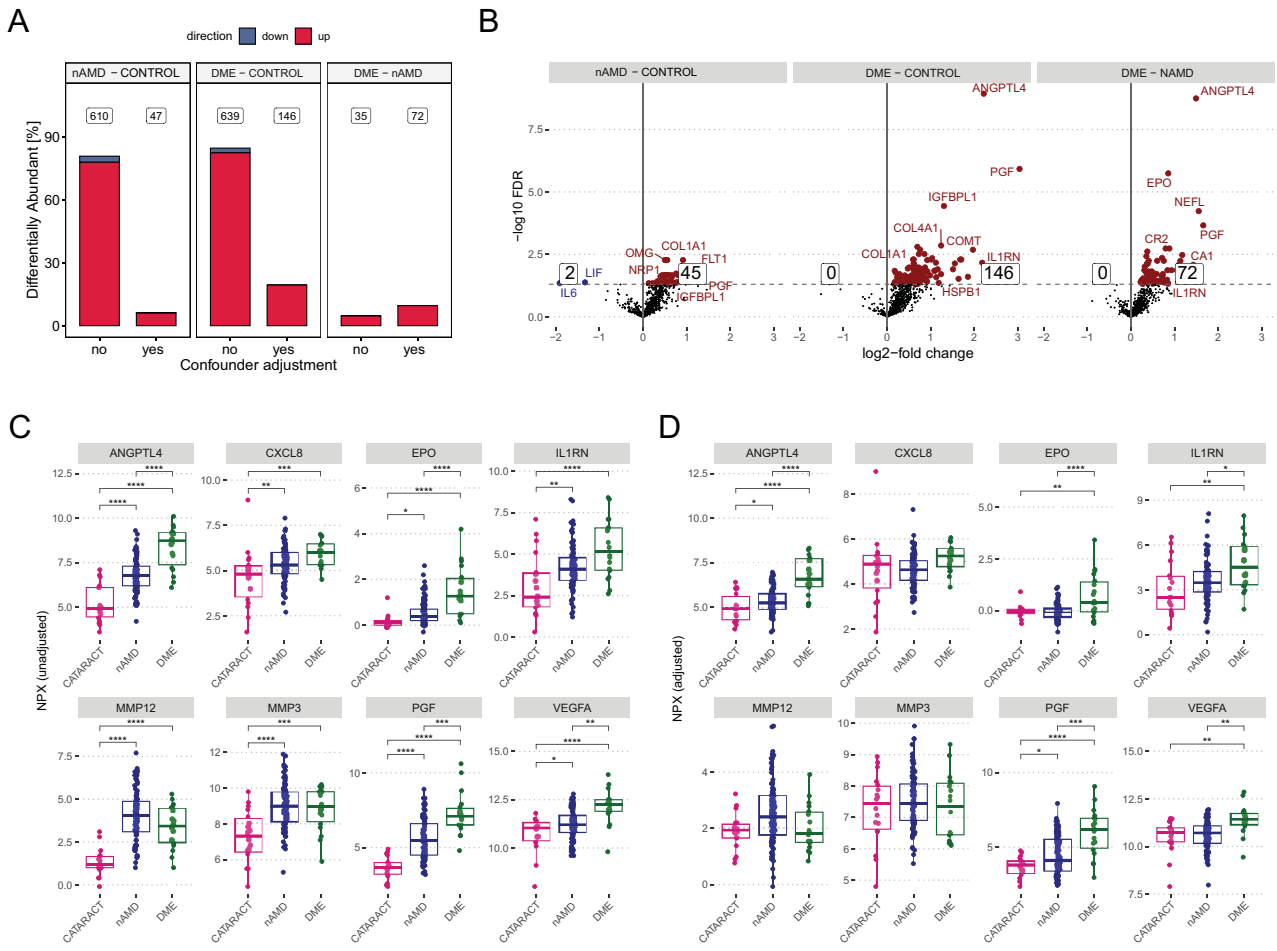

Figure 5. Covariate-adjusted differential protein abundance in aqueous humor. (**A**) Comparison of percentages of differentially abundant proteins before and after adjustment for lens status, protein concentration, and 3-hydroxymandelate exposure in the three group comparisons (FDR < 0.05). Upregulated proteins are shown in *red*, downregulated proteins in *blue*. Absolute numbers of differentially abundant proteins are indicated. (**B**) Volcano plot showing the magnitude of effect (log_2 fold change on the *x*-axis) against the statistical significance ($–log_{10}$ FDR-adjusted *P* values on the *y*-axis) for the covariate-adjusted analysis. See Supplementary Table S8 for details. (**C**) Box plots depict unadjusted protein quantities (NPX values) for select proteins, with individual data points and statistical significance markers (*FDR < 0.05, **FDR < 0.01, ***FDR < 0.001, ****FDR < 0.0001). (**D**) Adjusted box plots for the same proteins as in (**D**), controlling for the three ocular confounders.

group. Further analysis across a range of models revealed that protein concentration adjustment had the most substantial impact on the number of differentially abundant proteins, especially in the nAMD versus control and DME versus control comparisons (Supplementary Fig. S4).

We also examined whether proteins known to be associated with AMD or DR were overrepresented among the upregulated proteins in the AMD and DME groups (Supplementary Fig. S5A). No enrichment was observed in the unadjusted comparisons, which was expected due to the large percentage of differentially abundant proteins. However, for the adjusted comparisons, we observed a clear enrichment of AMD- and DR-associated proteins, with greater enrichment correlating with stronger disease-association scores. Of note, the unadjusted model showed higher enrichment in the DME versus nAMD comparison. The biological significance of these additional proteins warrants further investigation. Supplementary Figure S5B summarizes the disease-associated proteins identified in the fully adjusted model.

Figures 5C and 5D illustrate the differential abundance of selected proteins between unadjusted and fully adjusted models. For example, MMP12 and MMP3, significantly influenced by lens status, lost their differential significance after adjustment. In contrast, proteins such as angiopoietin-related protein 4 (ANGPTL4) and erythropoietin (EPO), known to be

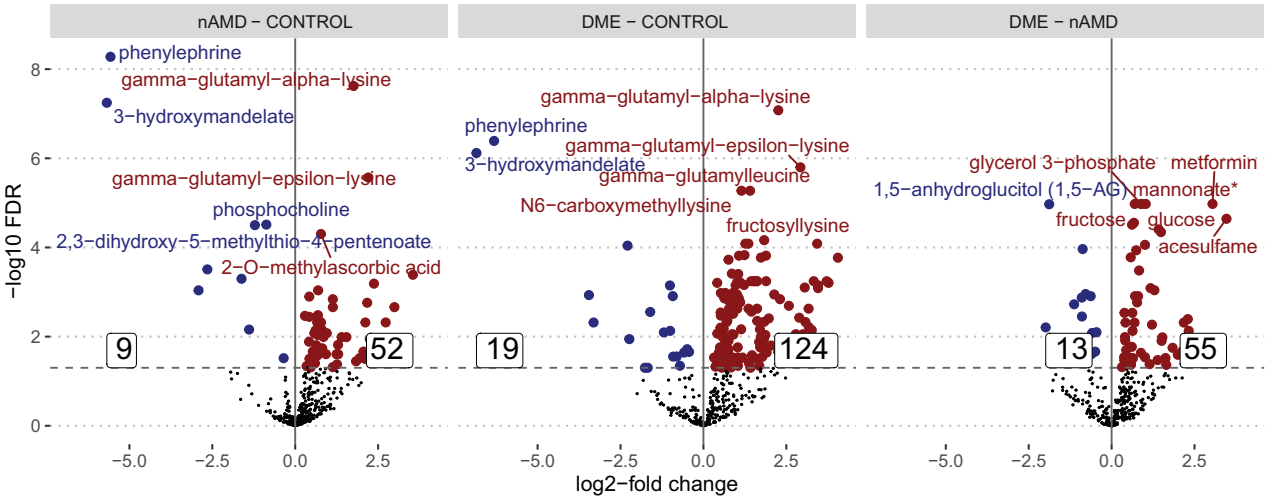

Figure 6. Differential metabolite abundance profiles in AH. Volcano plot shows the magnitude of effect (log_2 fold change on the *x*-axis) against the statistical significance ($-log_{10}$ FDR-adjusted *P* values on the *y*-axis). See Supplementary Table S9 for details.

associated with DR and DME, maintained or showed clearer differences post-adjustment.

In summary, accounting for identified confounders is crucial in the differential abundance analysis of AH proteins. However, the choice of adjustment should be guided by the specific biological questions at hand.

Differential Metabolite Abundance Analysis

Unlike AH proteins, metabolites in AH did not exhibit a strong, uniform positive correlation, as shown in Supplementary Figure S6. Consequently, the importance of confounder adjustment when analyzing metabolites is less evident. Therefore, we proceeded with unadjusted differential abundance analyses for metabolites (Fig. 6). For example, elevated glucose and fructose levels in patients with DME, along with decreased 1,5-anhydroglucitol, suggest poor glycemic control and chronic hyperglycemia. Additionally, the presence of metformin in the AH of patients with DME reflects its common use in type 2 diabetes management. It is worth noting, that two metabolites, gamma-glutamyl-alpha-lysine and gamma-glutamyl-epsilon-lysine, were markedly and significantly elevated in patients with nAMD and DME compared to controls, whereas phenylephrine and 3-hydroxymandelate levels were significantly higher in controls than in patients with nAMD or DME.

Discussion

In this study, we established comprehensive protein and metabolite profiles in AH samples from patients with DME, patients with nAMD, and patients undergoing cataract surgery without any retinal disease as controls. We could reliably quantify 756 proteins and 408 metabolites using the Olink Target 96 platform and Metabolon's LC-MS/MS platform, respectively. Before conducting an analysis to identify molecular factors that show differential abundance among controls and DME and nAMD patient groups, we examined the impact of total AH protein concentration and lens status on the analysis. Our investigation confirmed that these confounding factors can significantly influence the proteomic analyses of AH samples, in particular, and must be considered. Notably, we identified another yet unknown confounding factor, related to the use of phenylephrine for mydriasis, which also must be considered, particularly when exploring IL-6–related pathways in AH.

AH Protein Concentration

Previous research has indicated a link between higher protein levels in the AH and retinal diseases including DME and nAMD.[52,53] Consistent with these earlier reports, our data revealed that AH samples from patients with nAMD and DME contained remarkably increased total protein levels when compared to those from the control group. Both nAMD and DME are characterized by an impaired blood–retinal barrier (BRB), which is believed to account for the increased protein levels observed in the AH of these patients.[33–36,54,55] However, a recent proteomic profiling investigation, which compared paired samples of AH and serum, revealed that these two matrices are distinctly different.[10] This finding held true even in patients with DR, indicating that vascular leakage

of peripheral proteins does not substantially influence the AH proteome, even in diseases characterized by a compromised BRB. Moreover, several recent studies have demonstrated that, despite repeated anti-VEGF IVTs, AH protein levels remained elevated in patients with nAMD.[56–58] Our data further support this finding, indicating that the total concentration of AH protein does not significantly change from the time of diagnosis, particularly in patients with nAMD. Altogether, these findings imply that factors other than vascular leakage may contribute to the accumulation of proteins in the AH of patients with DME and nAMD. For example, ischemia (reduced blood flow) and hypoxia (low oxygen levels) are also associated with both conditions, prompting the release of various factors, including proteins, as part of the cellular response to stress.[59–64] Inflammatory responses, also distinctive features of nAMD and DME, result in cellular upregulation of cytokines, chemokines, growth factors, and MMPs—key contributors to retinal disease pathology.[36,64–69] The accumulation of age- and/or stress-induced senescent cells in the retinas of patients with nAMD and DME may provide another source for increased protein secretion. Senescent cells secrete numerous proteases, cytokines, and growth factors, termed the senescence-associated secretory phenotype, which can lead to inflammation, angiogenesis, and tissue remodeling.[70–73] The sum of events outlined can lead to a significant increase in proteins within the VH. Subsequently, upon diffusion into the AH, these proteins are highly likely to be a significant contributing factor to the observed heightened AH protein concentrations in DME and nAMD.

Lens Status

Prior research already acknowledges the impact of lens status (pseudophakic vs. phakic eyes) on AH protein concentration and composition.[29–32] Our analysis confirmed higher protein concentration in pseudophakic eyes compared to phakic eyes, especially in nAMD. Though a similar trend was seen in DME, statistical significance was not reached, likely due to smaller sample size. Phakic patients with nAMD and DME continue to demonstrate notably elevated levels of AH proteins compared to controls, underscoring that factors beyond lens status, as discussed earlier, play a substantial role in the observed protein variations.

What are the possible explanations for the effect of lens status on AH protein content? First, we must consider why pseudophakic eyes have higher protein concentrations in the AH. One hypothesis is that the natural lens in phakic eyes may act as a partial barrier to the diffusion of proteins from the VH to the AH, whereas, in pseudophakic eyes, the artificial intraocular lens (IOL) may not provide the same level of restriction. Supporting this, previous research has indicated that molecules can exit the vitreous into the anterior chamber via slow diffusion and that protein levels in the AH and VH can correlate due to this diffusion process.[10,74–78] From an anatomic perspective, the zonular tension and mechanical integrity may be compromised in response to a significantly thinner IOL compared with the natural lens, which corresponds with a reduced zonular resistance allowing an increased bidirectional fluid shift between the AH and VH. The differences in AH protein concentrations between phakic and pseudophakic patients can potentially also be explained by the findings of Neal and colleagues,[79] who observed marked differences in the viscosity of vitreous fluid in pseudophakic donor eyes compared to matched phakic donor eyes. These noted differences suggest that the status of the lens can directly impact the VH matrix, potentially influencing the protein diffusion from the VH to the AH. Overall, a reduced diffusion barrier property of the IOL compared to the natural lens and/or a change in the viscosity of the VH mediated by the IOL could potentially ease the diffusion of proteins from the VH into AH in pseudophakic patients. Presumably, this might also explain why the overall protein distinctions between pseudophakic patients with nAMD and phakic controls are more prominent than those between phakic patients with nAMD and phakic controls.

Of note, consistent with previous studies, our data also support persistent elevation of protein levels in pseudophakic patients post-cataract surgery (Supplementary Fig. S7).[31,32,80] This suggests that there are permanent changes in the protein concentration of the AH, possibly caused by pseudophakia-induced modifications in protein diffusion from the VH to the AH, as opposed to temporary shifts caused by surgery.

Notably, beyond the overall impact of the lens status on AH protein concentration, we identified a set of proteins that are likely expressed as a result of lens replacement. Differential abundance analysis revealed a significant association between pseudophakic lenses and increased levels of extracellular matrix (ECM)-related proteins such as MMPs, SERPINE1, and MFAP, alongside signaling mediators such as GDF15, CXCL10, and FGF19. GSEA results support the upregulation of ECM and intercellular signaling gene sets in pseudophakic eyes. Conversely, carbonic anhydrase 4 (CA4) showed decreased association with pseudophakia.

The positive association between pseudophakia and ECM-related proteins suggests increased ECM remodeling, whereas elevated signaling mediators imply enhanced intercellular signaling pathways. These alterations may potentially reflect the response of resid-

ual lens epithelial cells that endured the surgical lens-removal process. These cells can initiate a wound-healing response, such that cells can grow on capsular surfaces and occasionally the IOL.[81,82] This cellular growth is typically associated with fibrotic responses, where some cells undergo transdifferentiation into myofibroblasts, enhance matrix production, and induce matrix contraction.[81–83] In contrast, the observed lower abundance of CA4 in pseudophakic eyes, which is highly expressed in lens epithelial and fiber cells,[84] can be explained directly by the removal of the natural lens.

In summary, our findings underscore the intricate relationship between lens status and AH molecular composition in retinal diseases, emphasizing the importance of considering lens status in AH protein evaluations.

Phenylephrine/Tropicamide Administration

Unexpectedly, our analysis revealed significantly higher IL-6 levels in controls compared to those in patients with nAMD and DME. This contradicts established evidence that supports elevated IL-6 levels in the AH of patients with DME and nAMD compared to controls.[65,85–87]

Notably, our findings revealed that patients with elevated IL-6 levels showed increased levels of 3-hydroxymandelate, a primary metabolite of phenylephrine. Although 3-hydroxymandelate exhibited a strong correlation with phenylephrine, its detection in AH samples proved more consistent compared to phenylephrine levels. This difference could stem from either the relatively brief half-life of phenylephrine in AH or analytical factors.

Phenylephrine, recognized as a selective α-1 adrenergic receptor agonist with potent vasoconstrictive properties, is frequently employed in conjunction with tropicamide, a parasympathomimetic antagonist, as a mydriatic in ophthalmology.[88–90] Although each drug independently induces mydriasis, their combined application results in a more pronounced and light-resistant pupil dilation, especially advantageous under the bright illumination of an operating microscope.[91–93] The combination of 0.5% tropicamide and 2.5% phenylephrine in an eye drop formulation, as used in our study, is standard for achieving pupillary mydriasis before cataract surgery and is also frequently administered prior to fundus examinations and vitreoretinal surgeries.[94–96] Even before anti-VEGF IVTs, pupil dilation is usually performed to enable a swift examination of the retina in case of IVT-associated side effects.

Notably, elevated 3-hydroxymandelate levels were observed predominantly in control subjects from one study site. This site utilized Mydriasert (Thea Pharma, Lexington, MA), an ophthalmic pellet comprised of 0.28 mg tropicamide and 5.4 mg phenylephrine hydrochloride, placed in the lower conjunctival fornix 2 hours before cataract surgery and AH sampling. Mydriasert induces consistent and broad mydriasis through the gradual release of phenylephrine and tropicamide from the pellet. In contrast, at least two of the control subjects with low 3-hydroxymandelate levels were from a different study location, which exclusively employed 0.5% tropicamide and 2.5% phenylephrine–containing eye drops 10 to 30 minutes prior to cataract surgery and AH sampling. Expanding our analysis to patients with nAMD with elevated 3-hydroxymandelate levels demonstrated a similar effect on IL-6, very likely explaining the high IL-6 levels observed in this group. Upon investigation, it was revealed that patients with nAMD exhibiting highly elevated IL-6 levels had received eye drops containing 0.5% tropicamide and 2.5% phenylephrine 60 to 180 minutes before AH collection. The increased exposure to the mydriatic drugs before AH sampling occurred because these patients underwent retinal examinations, necessitating proper pupil dilation beforehand. The overall correlation observed between 3-hydroxymandelate and IL-6 levels in all patients suggests a positive relationship between the duration of exposure to the mydriatic drugs and AH IL-6 levels at the time of sampling. Unfortunately, precise details regarding the number of dilating drops administered and the interval between their application and AH sample collection are unavailable.

Currently, we are unable to definitively conclude whether the process of pupil dilation induced by mydriatic drugs itself prompts IL-6 elevation, potentially through mechanisms akin to "biomechanical stress." Alternatively, it remains plausible that phenylephrine and/or tropicamide (the latter drug could not be detected by the analytical method used in this study) may directly contribute to increased IL-6 levels in the AH. Supporting the latter hypothesis, there is existing data illustrating that phenylephrine elevated IL-6 mRNA levels in cultured astrocytes from the rat spinal cord, an effect mediated through activation of the α-1 adrenoceptor and involving the protein kinase C/extracellular signal-regulated kinase pathway.[97] The wide distribution of adrenoceptors in the eye, particularly in the smooth muscle cells of the iris, the blood vessels of the conjunctiva, and the ciliary processes, as well as the aqueous outflow tract,[98] further underscores the potential direct influence of phenylephrine on AH IL-6 levels.

In addition to IL-6, which showed the strongest response, we found that ezrin, G-CSF/CSF3, the IL-

6 family cytokine OSM, and the tissue repair factor amphiregulin were also significantly elevated in the high 3-hydroxymandelate nAMD group. Moreover, GSEA provided further insights, indicating a biological impact of phenylephrine/tropicamide exposure on pathways related to IL-6 family signaling and cytokine pathways. Although the DME group included only two cases with elevated 3-hydroxymandelate levels, the gene-set responses, including those for IL-6 signaling, paralleled those observed in the control and nAMD groups.

In conclusion, our data strongly suggest a potential link between ocular phenylephrine/tropicamide exposure and IL-6 secretion in the AH. This observation holds significant implications for AH biomarker interpretation, particularly in conditions such as DR, nAMD, uveitis, and retinal vein occlusion, where IL-6 is considered a strong biomarker of inflammation.[65,80,85,87,99–101] The unexpected elevation of IL-6 (and other factors) in the AH warrants further investigation to elucidate the dose–response relationship, temporal kinetics, and underlying mechanisms of this ocular tissue response. Moreover, further research is needed to comprehensively understand the clinical implications and to refine the application of phenylephrine/tropicamide-containing pupil-dilating drugs in ophthalmic procedures, particularly if sampling of intraocular fluids for biomarker research is attempted.

Considerations for Correlation Analyses

We identified a very strong positive correlation among most AH proteins analyzed, likely influenced by the variance in total protein concentration, as well as other confounding factors, observed across various patients and patient groups. Although specific protein correlation clusters were already visible in the unadjusted data, the pervasive correlation with total AH protein levels masks specific biological association between proteins. Notably, this becomes particularly significant for studies that assess only a limited number of AH proteins, as limited data may lead to incorrect biological assumptions about the importance of certain protein–protein relationships.

To address this, we adjusted the dataset for confounding factors, including lens status, protein concentration, and 3-hydroxymandelate levels. Following adjustment, the data presented a more defined correlation pattern, with several distinct protein clusters emerging among the three study groups. Notably, we discovered correlation clusters that were consistent between the nAMD and DME groups. Gene-set analysis indicated potential links between biological categories and these clusters. For example, we found a cluster enriched for neuronal proteins and another for metabolic enzymes that were common to both groups. In contrast, metabolites within the AH did not demonstrate a consistent positive correlation, suggesting that the adjustment for ocular confounders is less pertinent for metabolite data than for protein data.

Considerations for Differential Abundance Analyses

Addressing confounders is crucial in statistical analysis to ensure reproducible results and to uncover relevant patterns. In the current study, we focused on the three identified ocular factors—lens status, protein concentration, and 3-hydroxymandelate levels—that significantly affect protein levels in AH. Clearly, it is important to consider these factors to understand the biological processes of interest. However, the method of correction can differ depending on the research question and other scientific considerations. For example, it is important to recognize that, although certain cytokines may exhibit increased levels in parallel with overall protein concentration, this elevation could be biologically meaningful and indicative of inflammatory disease processes. Therefore, simply normalizing cytokine concentrations to protein levels without considering the biological context may obscure crucial insights into disease mechanisms. Similarly, separately looking at differences between patients with natural and artificial lenses can provide insights into these specific conditions. Keeping this diversity of possible approaches in mind, in the current manuscript we have evaluated how direct adjustment of these ocular factors affects the identification of differentially abundant proteins between the three study groups.

Given the pronounced differences between the control and retinal disease groups (nAMD and DME), the substantial decrease in differentially abundant proteins after adjusting for confounders in the control group comparisons was anticipated. For example, the number of differentially abundant proteins in the nAMD versus control groups comparison dropped from 610 to 47 following adjustment. Protein concentration was identified as the most impactful confounder. Prior to adjustment, our differential abundance analysis did not reveal any significant disease-related biological patterns. However, post-adjustment, there was a marked increase in proteins associated with AMD and DR, particularly those with strong disease associations in the Open Targets database.[50] These results highlight the critical role

of confounder adjustment for revealing meaningful biological insights from AH protein data.

As examples, we identified upregulation in DME versus nAMD and in DME versus controls of EPO, interleukin-1 receptor antagonist protein (IL1RN), and ANGPTL4. Hypoxia induces EPO expression in several retinal cell types[102] and previous studies identified elevated EPO levels in aqueous and vitreous humor associated with DR.[103,104] Functionally, dual roles have been proposed for EPO in retinal protection and pathological neovascularization.[102] Treatment of DR with the EPO protein has also been explored in a clinical study setting.[102] IL1RN is an IL-1 receptor antagonist and is used in recombinant form, as the drug anakinra, to treat inflammatory conditions in the clinic.[105] The contribution of IL-1β signaling to the pathogenesis of DR has been suggested by several preclinical studies; for example, in rodent models, anakinra treatment reduced the development of new subretinal vessels in laser-induced choroidal neovascularization models[106,107] and improved endothelial dysfunction in streptozocin-induced diabetic rats.[108] Finally, ANGPTL4 has been associated with DR severity and may influence vascular permeability, potentially contributing to macular edema.[109,110] The individual protein profiles of these examples clearly illustrate that confounder adjustment can help to more clearly highlight specific protein associations—in these cases, with DR/DME—and exclude clear confounder driven effects such as elevation of MMP12 in pseudophakic eyes.

Unlike AH proteins, AH metabolites demonstrated neither strongly positive correlation profiles nor such general associations with the identified confounding factors, which could be due to differences in turnover rates, diffusion properties, ocular clearance pathways, and/or the complex nature of metabolic pathways. Therefore, the need to adjust for the identified confounding factors is less evident for metabolites. In the unadjusted comparisons, the metabolic dysregulation in DME versus nAMD was evident, with increased glucose, mannonate, fructose, and glycerol-3-phosphate levels suggesting insufficiently controlled diabetes and chronic hyperglycemia. The reduction in 1,5-anhydroglucitol (1,5-AG) levels in the AH of DME patients is noteworthy. 1,5-AG serves as a short-term glycemic marker, like hemoglobin A1C (HbA1C) in blood but is less effective at extreme blood sugar levels.[111] Low 1,5-AG correlates with DR in moderately controlled diabetes (HbA1c $< 8\%$),[112] hinting at a role for glucose fluctuations in microvascular complications. Therefore, 1,5-AG may be a useful AH biomarker for evaluating the impact of chronic hyperglycemia, especially when HbA1C data are unavailable. Remarkably, two metabolites, gamma-glutamyl-alpha-lysine and gamma-glutamyl-epsilon-lysine, exhibited substantial and statistically significant elevation in patients with nAMD and DME when contrasted with controls. These metabolites are classified within the gamma-glutamyl dipeptides group, acknowledged as bioactive peptides intricately involved in processes such as inflammation, oxidative stress, and glucose regulation,[113] thus suggesting their potential utility as biomarkers for these disease conditions. The levels of 3-hydroxymandelate and phenylephrine were significantly higher in the controls compared to those with nAMD or DME, as previously discussed.

Study Limitations

Our investigation was subject to several limitations that warrant mention. Our study, although comprehensive with 138 patients, faced limitations in the distribution of participants across disease groups. The control and DME cohorts included only 18 patients each. The smaller size of the DME group, in particular, was an unforeseen consequence of the COVID-19 pandemic, which inadvertently led to a higher enrollment of patients with nAMD. This imbalance has restricted our ability to discern and compare the nuances between the nAMD and DME groups with the desired statistical robustness (e.g., see Supplementary Figure S1 for a power estimation of the lens status effect on AH protein concentrations). Moreover, the inclusion of patients already undergoing anti-VEGF IVT, with limited information available about the prior treatment duration and frequency, presented a challenge. It made distinguishing between disease-related and treatment-induced changes in the AH profiles difficult, prompting us to exercise caution in interpreting the data. To mitigate this, future research will aim to recruit treatment-naïve patients and track their molecular profiles longitudinally after treatment initiation to better isolate the effects of the disease from those of the therapy. Moreover, although the Olink Target 96 and Metabolon's LC-MS/MS platforms provide reliable targeted relative quantification, they do not offer absolute quantification for proteins and metabolites. The lower total protein concentration in the control group likely affected our ability to accurately quantify some of the proteins with lowest abundance in AH, possibly resulting in lower than expected effect sizes for these proteins. Finally, although we have demonstrated the impact of adjustment of the three identified ocular confounding factors directly in the linear statistical modeling approaches, other approaches can be taken and, likely, additional factors affecting the molecular composition of AH exist. Although we do not expect a strong risk of statistical adjustment bias introduced by the partial collinear-

ity between the lens status and AH protein concentration, it is still important to be aware of potential multicollinearity effects, such as when interpreting the coefficients of such collinear factors. Also, depending on the study questions, it might be relevant to only consider a subset of the identified confounders, such as if the biological impact of a disease-associated increase in total protein concentration is evaluated and other biological and/or demographic confounders could be considered.

Conclusions

In conclusion, our study emphasizes the importance of considering confounding factors such as AH protein concentration, lens status, and the effects of pupil dilation, mediated by phenylephrine/tropicamide, when analyzing AH proteins in the context of ocular diseases. Adjusting for these variables enabled a more stringent identification of disease-specific alterations and the establishment of potential links between AH protein profiles and their functional origins. Although our study identifies some constraints in employing AH as a substitute matrix for VH, it also presents practical approaches to enhance the accuracy of analyses conducted using AH, particularly in phakic patients, thereby better reflecting the conditions in the posterior segment of the eye. The translational relevance of our findings is significant, as they not only confirm AH as a viable source of protein biomarkers for retinal diseases but also highlight the necessity for meticulous consideration of confounding factors in both comprehensive proteomics studies and targeted bioanalytical protein measurements. This approach paves the way for more accurate biomarker discovery and the potential development of novel therapeutic strategies for ocular pathologies.

Acknowledgments

The authors thank Thu Le von Strauss, Mariana de Wouters, Patrick Cech, Vikki Green, Christin Schild, and Elmar Hulliger for their support in setting up the studies and collecting and preparing the biological samples. Initial language editing was assisted by OpenAI GPT-3.5/4 large language models executed within a dedicated Microsoft Azure instance. We also thank Katie Patel and Emmanuel Nussbaumer for data transfer–related support, Andreas Wenzel for reviewing the manuscript, and Louise Smyth for English language editing.

Supported by F. Hoffmann-La Roche Ltd.

Disclosure: **B. Titz**, F. Hoffmann-La Roche (E, I); **J. Siebourg-Polster**, F. Hoffmann-La Roche (E, I); **F. Bartolo**, Roche (C); **V. Lavergne**, Roche (C); **Z. Jiang**, F. Hoffmann-La Roche (E); **J. Gayan**, F. Hoffmann-La Roche (E, I); **L. Altay**, F. Hoffmann-La Roche (R, F), Apellis (R), AbbVie (R), Bayer (R), Novartis (R); **P. Enders**, F. Hoffmann-La Roche (C); **C. Schmelzeisen**, None; **Q.-T. Ippisch**, None; **M.J. Koss**, F. Hoffmann-La Roche (C); **S. Ansari-Shahrezaei**, F. Hoffmann-La Roche (C, F), AbbVie (C), Apellis (C), Bayer (C, F), Novartis (C); **J.G. Garweg**, AbbVie (R), Bayer (R), Novartis (C, R), F. Hoffmann-La Roche (C, R); **S. Fauser**, F. Hoffmann-La Roche (E, I); **A. Dieckmann**, F. Hoffmann-La Roche (E, I)

* BT and JSP contributed equally to this article.

References

1. Monteiro JP, Santos FM, Rocha AS, et al. Vitreous humor in the pathologic scope: insights from proteomic approaches. *Proteom Clin Appl*. 2015;9(1–2):187–202.
2. der Lelij AV, Rothova A. Diagnostic anterior chamber paracentesis in uveitis: a safe procedure? *Br J Ophthalmol*. 1997;81(11):976–979.
3. Saxena S, Lai TY, Koizumi H, et al. Anterior chamber paracentesis during intravitreal injections in observational trials: effectiveness and safety and effects. *Int J Retin Vitr*. 2019;5(1):8.
4. Balaiya S, Zhou Z, Chalam KV. Characterization of vitreous and aqueous proteome in humans with proliferative diabetic retinopathy and its clinical correlation. *Proteom Insights*. 2017;8:1178641816686078.
5. Funatsu H, Yamashita H, Noma H, et al. Aqueous humor levels of cytokines are related to vitreous levels and progression of diabetic retinopathy in diabetic patients. *Graefes Arch Clin Exp Ophthalmol*. 2005;243(1):3–8.
6. Noma H, Funatsu H, Yamasaki M, et al. Aqueous humour levels of cytokines are correlated to vitreous levels and severity of macular oedema in branch retinal vein occlusion. *Eye (Lond)*. 2008;22(1):42–48.
7. Smith JM, Mandava N, Tirado-Gonzalez V, et al. Correlation of complement activation in aqueous and vitreous in patients with proliferative diabetic retinopathy. *Transl Vis Sci Technol*. 2022;11(4):13.

8. Wang Y, Gao S, Zhu Y, Shen X. Elevated activating transcription factor 4 and glucose-regulated 78 Kda protein levels correlate with inflammatory cytokines in the aqueous humor and vitreous of proliferative diabetic retinopathy. *Curr Eye Res*. 2017;42(8):1202–1208.
9. Wu F, Phone A, Lamy R, et al. Correlation of aqueous, vitreous, and plasma cytokine levels in patients with proliferative diabetic retinopathy. *Invest Ophthalmol Vis Sci*. 2020;61(2):26.
10. Wilson S, Siebourg-Polster J, Titz B, et al. Correlation of aqueous, vitreous, and serum protein levels in patients with *retina*l diseases. *Transl Vis Sci Technol*. 2023;12(11):9.
11. Fauser S, Schwabecker V, Muether PS. Suppression of intraocular vascular endothelial growth factor during aflibercept treatment of age-related macular degeneration. *Am J Ophthalmol*. 2014;158(3):532–536.
12. Minaker SA, Mason RH, Luna GL, Bapat P, Muni RH. Changes in aqueous and vitreous inflammatory cytokine levels in neovascular age-related macular degeneration: a systematic review and meta-analysis. *Acta Ophthalmol*. 2021;99(2):134–155.
13. Minaker SA, Mason RH, Luna GL, et al. Changes in aqueous and vitreous inflammatory cytokine levels in diabetic macular oedema: a systematic review and meta-analysis. *Acta Ophthalmol*. 2022;100(1):e53–e70.
14. Kodeboyina SK, Lee TJ, Churchwell L, et al. The constitutive proteome of human aqueous humor and race specific alterations. *Proteomes*. 2020;8(4):34.
15. Yu M, Xie F, Liu X, et al. Proteomic study of aqueous humor and its application in the treatment of neovascular glaucoma. *Front Mol Biosci*. 2020;7:587677.
16. Kim TW, Kang JW, Ahn J, et al. Proteomic analysis of the aqueous humor in age-related macular degeneration (AMD) patients. *J Proteome Res*. 2012;11(8):4034–4043.
17. Velez G, Tang PH, Cabral T, et al. Personalized proteomics for precision health: identifying biomarkers of vitreoretinal disease. *Transl Vis Sci Technol*. 2018;7(5):12.
18. Chowdhury UR, Madden BJ, Charlesworth MC, Fautsch MP. Proteome analysis of human aqueous humor. *Invest Ophthalmol Vis Sci*. 2010;51(10):4921.
19. Murthy KR, Rajagopalan P, Pinto SM, et al. Proteomics of human aqueous humor. *OMICS*. 2015;19(5):283–293.
20. Nobl M, Reich M, Dacheva I, et al. Proteomics of vitreous in neovascular age-related macular degeneration. *Exp Eye Res*. 2016;146:107–117.
21. Koss MJ, Hoffmann J, Nguyen N, et al. Proteomics of vitreous humor of patients with exudative age-related macular degeneration. *PLoS One*. 2014;9(5):e96895.
22. Assarsson E, Lundberg M, Holmquist G, et al. Homogenous 96-plex PEA immunoassay exhibiting high sensitivity, specificity, and excellent scalability. *PLoS One*. 2014;9(4):e95192.
23. Wang H, Fang J, Chen F, et al. Metabolomic profile of diabetic retinopathy: a GC-TOFMS-based approach using vitreous and aqueous humor. *Acta Diabetol*. 2020;57(1):41–51.
24. Xiong X, Chen X, Ma H, et al. Metabolite changes in the aqueous humor of patients with retinal vein occlusion macular edema: a metabolomics analysis. *Front Cell Dev Biol*. 2021;9:762500.
25. Jiang D, Yan C, Ge L, et al. Metabolomic analysis of aqueous humor reveals potential metabolite biomarkers for differential detection of macular edema. *Eye Vis*. 2023;10(1):14.
26. Pan CW, Ke C, Chen Q, et al. Differential metabolic markers associated with primary open-angle glaucoma and cataract in human aqueous humor. *BMC Ophthalmol*. 2020;20(1):183.
27. Tokarz J, Adamski J. Confounders in metabolomics. In: Adamski J, ed. *Metabolomics for Biomedical Research*. Cambridge, MA: Academic Press; 2020:17–32.
28. Schork K, Podwojski K, Turewicz M, Stephan C, Eisenacher M. Quantitative methods in proteomics. *Methods Mol Biol*. 2021;2228:1–20.
29. Schoeneberger V, Eberhardt S, Menghesha L, Enders P, Cursiefen C, Schaub F. Association between blood-aqueous barrier disruption and extent of retinal detachment. *Eur J Ophthalmol*. 2022;33(1):421–427.
30. Schoeneberger V, Menghesha L, Gerlach S, et al. Lens status and degree of lens opacity influence laser flare photometry (objective tyndallometry). *Eur J Ophthalmol*. 2022;33(2):943–948.
31. Maria MD, Coassin M, Mastrofilippo V, Cimino L, Iannetta D, Fontana L. Persistence of inflammation after uncomplicated cataract surgery: a 6-month laser flare photometry analysis. *Adv Ther*. 2020;37(7):3223–3233.
32. Schauersberger J, Kruger A, Müllner-Eidenböck A, et al. Long-term disorders of the blood-aqueous barrier after small-incision cataract surgery. *Eye (Lond)*. 2000;14(1):61–63.
33. Shoughy SS, Elkum N, Tabbara KF. Aqueous protein level and flare grading. *Acta Ophthalmol*. 2015;93(2):e173–e174.

34. Jandrasits K, Krepler K, Wedrich A. Aqueous flare and macular edema in eyes with diabetic retinopathy. *Ophthalmologica*. 2003;217(1):49–52.
35. Sawa M. Laser flare-cell photometer: principle and significance in clinical and basic ophthalmology. *Jpn J Ophthalmol*. 2017;61(1):21–42.
36. Noma H, Mimura T, Yasuda K, Shimura M. Role of inflammation in diabetic macular edema. *Ophthalmologica*. 2014;232(3):127–135.
37. Küchle M, Nguyen NX, Martus P, Freissler K, Schalnus R. Aqueous flare in retinitis pigmentosa. *Graefes Arch Clin Exp Ophthalmol*. 1998;236(6):426–433.
38. Kubota T, Motomatsu K, Sakamoto M, Honda T, Ishibashi T. Aqueous flare in eyes with senile disciform macular degeneration: correlation with clinical stage and area of neovascular membrane. *Graefes Arch Clin Exp Ophthalmol*. 1996;234(5):285–287.
39. Nguyen NX, Schönherr U, Küchle M. Aqueous flare and retinal capillary changes in eyes with diabetic retinopathy. *Ophthalmologica*. 1995;209(3):145–148.
40. Schröder S, Muether PS, Caramoy A, et al. Anterior chamber aqueous flare is a strong predictor for proliferative vitreoretinopathy in patients with rhegmatogenous retinal detachment. *Retina*. 2012;32(1):38–42.
41. Pfister IB, Zandi S, Gerhardt C, Spindler J, Reichen N, Garweg JG. Risks and challenges in interpreting simultaneous analyses of multiple cytokines. *Transl Vis Sci Technol*. 2020;9(7):27.
42. Ritchie ME, Phipson B, Wu D, et al. limma powers differential expression analyses for RNA-sequencing and microarray studies. *Nucleic Acids Res*. 2015;43(7):e47.
43. Lenth RV. Emmeans: estimated marginal means, aka least-squares means. Available at: https://CRAN.R-project.org/package=emmeans. Accessed June 12, 2024.
44. Wilkerson MD, Hayes DN. ConsensusClusterPlus: a class discovery tool with confidence assessments and item tracking. *Bioinformatics*. 2010;26(12):1572–1573.
45. Monti S, Tamayo P, Mesirov J, Golub T. Consensus clustering: a resampling-based method for class discovery and visualization of gene expression microarray data. *Mach Learn*. 2003;52(1–2):91–118.
46. Dolgalev I. msigdbr: MSigDB gene sets for multiple organisms in a tidy data format. Available at: https://cran.r-project.org/web/packages/msigdbr/msigdbr.pdf. Accessed June 12, 2024.
47. Liberzon A, Subramanian A, Pinchback R, Thorvaldsdóttir H, Tamayo P, Mesirov JP. Molecular signatures database (MSigDB) 3.0. *Bioinformatics*. 2011;27(12):1739–1740.
48. Szklarczyk D, Kirsch R, Koutrouli M, et al. The STRING database in 2023: protein–protein association networks and functional enrichment analyses for any sequenced genome of interest. *Nucleic Acids Res*. 2022;51(D1):D638–D646.
49. Väremo L, Nielsen J, Nookaew I. Enriching the gene set analysis of genome-wide data by incorporating directionality of gene expression and combining statistical hypotheses and methods. *Nucleic Acids Res*. 2013;41(8):4378–4391.
50. Ochoa D, Hercules A, Carmona M, et al. The next-generation Open Targets Platform: reimagined, redesigned, rebuilt. *Nucleic Acids Res*. 2022;51(D1):D1353–D1359.
51. Gelotte CK, Zimmerman BA. Pharmacokinetics, safety, and cardiovascular tolerability of phenylephrine HCl 10, 20, and 30 mg after a single oral administration in healthy volunteers. *Clin Drug Investig*. 2015;35(9):547–558.
52. Zaczek A, Hallnäs K, Zetterström C. Aqueous flare intensity in relation to different stages of diabetic retinopathy. *Eur J Ophthalmol*. 1999;9(3):158–164.
53. Kubota T, Küchle M, Nguyen NX. Aqueous flare in eyes with age-related macular degeneration. *Jpn J Ophthalmol*. 1994;38(1):67–70.
54. O'Leary F, Campbell M. The blood–retina barrier in health and disease. *FEBS J*. 2023;290(4):878–891.
55. Vinores SA. Breakdown of the blood–retinal barrier. In: Dartt DA, Besharse J, Dana R, et al., eds. *Encyclopedia of the Eye*. Cambridge, MA: Academic Press; 2010:216–222.
56. Dolar-Szczasny J, Bucolo C, Zweifel S, et al. Evaluation of aqueous flare intensity in eyes undergoing intravitreal bevacizumab therapy to treat neovascular age-related macular degeneration. *Front Pharmacol*. 2021;12:656774.
57. Matsubara H, Nagashima R, Chujo S, et al. Subclinical ocular changes after intravitreal injections of different anti-VEGF agents for neovascular age-related macular degeneration. *J Clin Med*. 2023;12(23):7401.
58. Motohashi R, Noma H, Yasuda K, Kasezawa Y, Goto H, Shimura M. Aqueous flare, functional-morphological parameters, and cytokines in age-related macular degeneration after anti-VEGF treatment. *Open Ophthalmol J*. 2021;15(1):209–216.
59. Mammadzada P, Corredoira PM, André H. The role of hypoxia-inducible factors in neovascular

age-related macular degeneration: a gene therapy perspective. *Cell Mol Life Sci*. 2020;77(5):819–833.
60. Campochiaro PA. Ocular neovascularization. *J Mol Med*. 2013;91(3):311–321.
61. de Freitas LGA, Isaac DLC, Abud MB, et al. Analysis of cytokines in the aqueous humor during intravitreal Ranibizumab treatment of diabetic macular edema. *Sci Rep*. 2021;11(1):23981.
62. Noma H, Yasuda K, Shimura M. Involvement of cytokines in the pathogenesis of diabetic macular edema. *Int J Mol Sci*. 2021;22(7):3427.
63. Campochiaro PA. Retinal and choroidal vascular diseases: past, present, and future: the 2021 Proctor Lecture. *Invest Ophthalmol Vis Sci*. 2021;62(14):26.
64. Dammak A, Huete-Toral F, Carpena-Torres C, Martin-Gil A, Pastrana C, Carracedo G. From oxidative stress to inflammation in the posterior ocular diseases: diagnosis and treatment. *Pharmaceutics*. 2021;13(9):1376.
65. Ghasemi H. Roles of IL-6 in ocular inflammation: a review. *Ocul Immunol Inflamm*. 2018;26(1):37–50.
66. Pongsachareonnont P, Mak MYK, Hurst CP, Lam WC. Neovascular age-related macular degeneration: intraocular inflammatory cytokines in the poor responder to ranibizumab treatment. *Clin Ophthalmol*. 2018;12:1877–1885.
67. Heloterä H, Kaarniranta K. A linkage between angiogenesis and inflammation in neovascular age-related macular degeneration. *Cells*. 2022;11(21):3453.
68. Arai Y, Takahashi H, Inoda S, et al. Aqueous humour proteins and treatment outcomes of anti-VEGF therapy in neovascular age-related macular degeneration. *PLoS One*. 2020;15(3):e0229342.
69. Vofo BN, Chowers I. Suppressing inflammation for the treatment of diabetic retinopathy and age-related macular degeneration: dazdotuftide as a potential new multitarget therapeutic candidate. *Biomedicines*. 2023;11(6):1562.
70. Fu Z, Smith LEH. Cellular senescence in pathologic retinal angiogenesis. *Trends Endocrinol Metab*. 2021;32(7):415–416.
71. Soleimani M, Cheraqpour K, Koganti R, Djalilian AR. Cellular senescence and ophthalmic diseases: narrative review. *Graefes Arch Clin Exp Ophthalmol*. 2023;261(11):3067–3082.
72. Sreekumar PG, Hinton DR, Kannan R. The emerging role of senescence in ocular disease. *Oxidative Med Cell Longev*. 2020;2020:2583601.
73. Crespo-Garcia S, Fournier F, Diaz-Marin R, et al. Therapeutic targeting of cellular senescence in diabetic macular edema: preclinical and phase 1 trial results. *Nat Med*. 2024;30(2):443–454.
74. Maurice DM. Flow of water between aqueous and vitreous compartments in the rabbit eye. *Am J Physiol*. 1987;252(1):F104–F108.
75. Xu Q, Boylan NJ, Suk JS, et al. Nanoparticle diffusion in, and microrheology of, the bovine vitreous ex vivo. *J Control Release*. 2013;167(1):76–84.
76. Martens TF, Vercauteren D, Forier K, et al. Measuring the intravitreal mobility of nanomedicines with single-particle tracking microscopy. *Nanomedicine (Lond)*. 2013;8(12):1955–1968.
77. Käsdorf BT, Arends F, Lieleg O. Diffusion regulation in the vitreous humor. *Biophys J*. 2015;109(10):2171–2181.
78. Shimada H, Akaza E, Yuzawa M, Kawashima M. Concentration gradient of vascular endothelial growth factor in the vitreous of eyes with diabetic macular edema. *Invest Ophthalmol Vis Sci*. 2009;50(6):2953.
79. Neal RE, Bettelheim FA, Lin C, Winn KC, Garland DL, Zigler JS. Alterations in human vitreous humour following cataract extraction. *Exp Eye Res*. 2005;80(3):337–347.
80. Jakobsson G, Sundelin K, Zetterberg H, Zetterberg M. Increased levels of inflammatory immune mediators in vitreous from pseudophakic eyes. *Invest Ophthalmol Vis Sci*. 2015;56(5):3407.
81. Wormstone IM, Wang L, Liu CSC. Posterior capsule opacification. *Exp Eye Res*. 2009;88(2):257–269.
82. Wormstone IM, Wormstone YM, Smith AJO, Eldred JA. Posterior capsule opacification: what's in the bag? *Prog Retin Eye Res*. 2021;82:100905.
83. Eldred JA, Dawes LJ, Wormstone IM. The lens as a model for fibrotic disease. *Philos Trans R Soc Lond B Biol Sci*. 2011;366(1568):1301–1319.
84. Hageman GS, Zhu XL, Waheed A, Sly WS. Localization of carbonic anhydrase IV in a specific capillary bed of the human eye. *Proc Natl Acad Sci USA*. 1991;88(7):2716–2720.
85. Mesquida M, Drawnel F, Fauser S. The role of inflammation in diabetic eye disease. *Semin Immunopathol*. 2019;41(4):427–445.
86. Wu J, Zhong Y, Yue S, et al. Aqueous humor mediator and cytokine aberrations in diabetic retinopathy and diabetic macular edema: a systematic review and meta-analysis. *Dis Markers*. 2019;2019:6928524.
87. Yi Q, Wang Y, Chen L, et al. Implication of inflammatory cytokines in the aqueous humour

for management of macular diseases. *Acta Ophthalmol*. 2020;98(3):e309–e315.
88. Meyer SM, Fraunfelder FT. 3. Phenylenhrine hydrochloride. *Ophthalmology*. 1980;87(11): 1177–1180.
89. Alpay A, Ugurbas SC, Aydemir C. Efficiency and safety of phenylephrine and tropicamide used in premature retinopathy: a prospective observational study. *BMC Pediatr*. 2019;19(1):415.
90. Levine L. Mydriatic effectiveness of dilute combinations of phenylephrine and tropicamide. *Am J Optom Physiol Opt*. 1982;59(7):580–594.
91. Eyeson-Annan ML, Hirst LW, Battistutta D, Green A. Comparative pupil dilation using phenylephrine alone or in combination with tropicamide. *Ophthalmology*. 1998;105(4):726–732.
92. Lux A, Degoumois A, Barjol A, Mouriaux F, Denion E. Combination of 5% phenylephrine and 0.5% tropicamide eyedrops for pupil dilation in neonates is twice as effective as 0.5% tropicamide eyedrops alone. *Acta Ophthalmol*. 2017;95(2):165–169.
93. Apt L, Henrick A. Pupillary dilatation with single eyedrop mydriatic combinations. *Am J Ophthalmol*. 1980;89(4):553–559.
94. Lam PT, Poon BT, Wu W, Chi SC, Lam DS. Randomized clinical trial of the efficacy and safety of tropicamide and phenylephrine in preoperative mydriasis for phacoemulsification. *Clin Exp Ophthalmol*. 2003;31(1):52–56.
95. Krumholz DM, Portello JK, Rosenfield M, Rosenbaum JD. A combination solution for routine pupillary dilation. *Optometry*. 2006;77(7):350–353.
96. Lodhi SAK, Ramsali MV, Kulkarni DK, Surender P, Murty S. Safety of tropicamide and phenylephrine in pupillary mydriasis for cataract surgery. *Saudi J Ophthalmol*. 2022;35(2):108–111.
97. Morimoto K, Eguchi R, Kitano T, Otsuguro K-I. Alpha and beta adrenoceptors activate interleukin-6 transcription through different pathways in cultured astrocytes from rat spinal cord. *Cytokine*. 2021;142:155497.
98. McAuliffe-Curtin D, Buckley C. Review of alpha adrenoceptor function in the eye. *Eye (Lond)*. 1989;3(4):472–476.
99. Wang B, Zhang X, Chen H, Koh A, Zhao C, Chen Y. A review of intraocular biomolecules in retinal vein occlusion: toward potential biomarkers for companion diagnostics. *Front Pharmacol*. 2022;13:859951.
100. Weinstein JE, Pepple KL. Cytokines in uveitis. *Curr Opin Ophthalmol*. 2018;29(3):267–274.
101. Minaker SA, Mason RH, Luna GL, et al. Changes in aqueous and vitreous inflammatory cytokine levels in diabetic macular oedema: a systematic review and meta-analysis. *Acta Ophthalmol*. 2022;100(1):e53–e70.
102. Feizi S, Alemzadeh-Ansari M, Karimian F, Esfandiari H. Use of erythropoietin in ophthalmology: a review. *Surv Ophthalmol*. 2022;67(2):427–439.
103. Pessoa B, Heitor J, Coelho C, et al. Systemic and vitreous biomarkers—new insights in diabetic retinopathy. *Graefes Arch Clin Exp Ophthalmol*. 2022;260(8):2449–2460.
104. Semeraro F, Cancarini A, Morescalchi F, et al. Serum and intraocular concentrations of erythropoietin and vascular endothelial growth factor in patients with type 2 diabetes and proliferative retinopathy. *Diabetes Metab*. 2014;40(6):445–451.
105. Migliorini P, Italiani P, Pratesi F, Puxeddu I, Boraschi D. The IL-1 family cytokines and receptors in autoimmune diseases. *Autoimmun Rev*. 2020;19(9):102617.
106. Olson JL, Courtney RJ, Rouhani B, Mandava N, Dinarello CA. Intravitreal anakinra inhibits choroidal neovascular membrane growth in a rat model. *Ocul Immunol Inflamm*. 2009;17(3):195–200.
107. Lavalette S, Raoul W, Houssier M, et al. Interleukin-1β inhibition prevents choroidal neovascularization and does not exacerbate photoreceptor degeneration. *Am J Pathol*. 2011;178(5):2416–2423.
108. Vallejo S, Palacios E, Romacho T, Villalobos L, Peiró C, Sánchez-Ferrer CF. The interleukin-1 receptor antagonist anakinra improves endothelial dysfunction in streptozotocin-induced diabetic rats. *Cardiovasc Diabetol*. 2014;13(1):158.
109. Babapoor-Farrokhran S, Jee K, Puchner B, et al. Angiopoietin-like 4 is a potent angiogenic factor and a novel therapeutic target for patients with proliferative diabetic retinopathy. *Proc Natl Acad Sci USA*. 2015;112(23):E3030–E3039.
110. Zhang Q, Qi S, You J, Wang C. The role of retinal glial cells and related factors in macular edema. *Biochem Biophys Res Commun*. 2024;695:149415.
111. Kim WJ, Park CY. 1,5-Anhydroglucitol in diabetes mellitus. *Endocrine*. 2013;43(1):33–40.
112. Kim WJ, Park CY, Park SE, et al. Serum 1,5-anhydroglucitol is associated with diabetic retinopathy in type 2 diabetes. *Diabet Med*. 2012;29(9):1184–1190.
113. Wu Q, Li J, Zhu J, et al. Gamma-glutamyl-leucine levels are causally associated with elevated cardiometabolic risks. *Front Nutr*. 2022;9:936220.